

Optimization of delamination resistance of vacuum infused glass laminate aluminum reinforced epoxy (GLARE) using various surface preparation techniques

Fathi A. Alshamma¹, Mustafa M. Kadhim²

^{1,2}Mechanical Department, College of Engineering, Baghdad University, Iraq

ABSTRACT

GLARE (glass laminate aluminum-reinforced epoxy) is aluminum-based material of fiber metal laminate (henceforth FML) that is often fabricated by expensive autoclave procedure. In this study, the process of Injected Molding (or also known as VARTM) was employed as a cost-effective alternative to produce GLARE. Several aluminum surface preparation procedures are applied to improve the interlaminar shear strength. A T3 temper 2024 aluminum alloy with 1*1 plain fabricated glass fabrics were used to make GLARE composites. GLARE consists of two aluminum sheet as external layers and glass fabric as internal layers. Four sets of aluminum sheets were prepared, one unanodized and three other anodized. Three different anodizing procedures (constant voltage mode, increasing voltage mode and decreasing voltage mode) have been adopted in this research. Two types of curing treatments were applied on VARTM fabricated specimens. According to ASTM D1876 T-peel test standard, the sets of prepared specimens have been tested to examine the adhesive bonding strength and fracture toughness of mode-I. The obtained results which include force-displacement curves, peak loads and fracture toughness were showed that a significant improvement for anodized specimens with all voltage modes. The first curing treatment offered better results than second curing treatment. The best improvement was obtained from anodized specimen with decreasing voltage mode cured by the first treatment which reaches to six times the results obtained from unanodized specimen. The delamination behavior for this specimen was verified numerically.

Keywords: GLARE, Aluminum, T-peel, VARTM, Adhesive bonding, surface treatments

Corresponding Author:

Mustafa Mohammed Kadhim
Mechanical Department, College of Engineering, Baghdad University
Baghdad, Iraq
Email: m.kadhim1803d@coeng.uobaghdad.edu.iq

1. Introduction

Recent trend in international research go toward developing, design and test high performance and light-weight material e.g. (FML) in aerospace and automotive fields to enhance crack propagation resistance and other over all mechanical properties [1-4]. FML is a composite material composed of several layers of high strength metal (aluminum, magnesium and titanium) which alternatively bonded with fiber composite layers [5, 6]. These advanced laminates offer superior resistance of fatigue crack propagation. They also offer significant resistance to corrosion and exert profound impact and low intensity. FML also show great tolerance of damage and ample damping qualities when compared with high performance aluminum alloy and other used metal [7]. The modification introduced in the used metallic alloy included the type as well as the quantity of this material. It also involved the number of metal and fiber layers, stacking sequence, fiber orientation and adhesive system (epoxy resin and hardener with different mixing ratio and curing processes), an extensive list of desirable characteristics can be obtained depending on the desired application [7, 8]. Researchers of Delft University of Technology Netherland discovered and developed the three most widely used forms of aluminum alloys- based fiber metal laminates in aircraft and automotive industry. These types, according to the date of their discovery namely are aramid fiber reinforced aluminum laminate, glass fiber laminate aluminum- reinforced epoxy in

addition to the aforementioned carbon fiber reinforced aluminum laminate, (the three also known as ARALL, GLARE and CARALL respectively) [9, 10]. In present days, FMLs are widely used in aerospace industry, such as in upper part of fuselage of Airbus A380, Boeing C-17 cargo hold door as well as Fokker 27 lower-wing-skin-stringer panels [11, 12]. Autoclave process is commonly used to manufacture fiber metal laminates. However, in the last few years, (VARTM) process gained more popularity as it is suitable to produce big part, free voids and hybrid cost-effective materials of top quality [13-17]. Prior to fiber metal laminate fabrication, several treatments on aluminum surface have been performed to increase the adhesive bonding strength. Aluminum surface treatments result in quite roughened and mechanically stable surface which is assist to maximize bonding area [18, 19]. In aerospace fields, processes such as degreasing, mechanical, chemical, electrolytic passivation (electrochemical or also known as anodizing) as well as chemical bonding agent and dry-state surface treating techniques are performed to improve aluminum surface and bonding system [20-22]. Many of researches studied the fatigue crack propagation resistance, mechanical properties, durability and interlaminar shear strength in order to improve FML performance and bonding interaction between aluminum surface and fiber layers [23-27]. This study explains all the steps of glass fiber reinforced aluminum laminate (GLARE) fabrication which includes surface treatments (degreasing, mechanical, chemical and electrochemical treatments), VARTM process and curing process with special interest on interface enhancement. Modification in electrochemical aluminum surface treatment is applied by using three different phosphoric acid anodizing voltage cycles. Six sets of specimens were prepared to measure and compare the effect of anodizing process and post-curing on interface reaction between aluminum and glass fiber layers. T-peel (ASTM D1876) test method was performed to gauge the peel resistance of the adhesive-bonded materials and assess the impact of anodizing and post-curing temperature on the aforementioned specimens.

2. Experimental procedure

The materials chosen for this study are described in this section. Aluminum surface preparation methods with modification, VARTM, infusion and curing techniques have also been described in this section.

2.1. Materials

2XXX series of aluminum alloy was chosen for GLARE fabrication. The main alloying constituents in 2XXX series aluminum alloy are copper (Cu) and magnesium (Mg). Because it's very good fatigue resistance, high corrosion resistance and low weight to strength factor, 2024 aluminum alloy is extensively used in aerospace field [28]. In this research, Aluminum Sheet/Plate 2024-T3 (0.3 mm in thickness) has been tested. Glass woven fabric 1*1 plain weave is used to fabricate GLARE laminate. The adhesive system consist of two components is epoxy resin L and hardener GL2 supplied by German company of composite technology was used in manufacturing GLARE 2/1. Long processing time, low viscosity and good mechanical properties make it appropriate for VARTM technique. Table 1 show the mechanical features of adhesive system, glass fabric and aluminum alloy sheet as provided by the supplier.

Table 1. Mechanical properties of GLARE materials

Name of material	T3 temper 2024 alloy	Glass fabric	Adhesive system
Grade	-	1*1 plane weave	Epoxy resin L / Hardener GL2 (210 min.)
Ultimate Tensile strength σ_u (megapascals or Mpa)	480	360	65 - 85
Elastic Modulus (gigapascals or Gpa)	72.4	33	3.4 – 3.8
Elongation ϕ (%)	14	4.86	1.4 – 2.3
Density ρ (g/cm ³)	2.78	2.55	0.98 – 1.19
Poisson ratio μ	0.33	0.3	0.32
Thickness t (mm)	0.3	0.32	-

2.2. Aluminum surface treatments

To get strong adhesive bonding with aluminum surface, several surface treatments were performed on aluminum sheets. Surface treatments can be detailed as follow:

2.2.1. Degreasing

To clean aluminum surface from the contamination such as dirt, grease and debris, aluminum sheets is dipped in acetone for 5 minutes, then the sheets are rinsed with distill water for several minutes. Degreasing process only removes impurities but cannot produce the required adhered surface conditions conducive to long-lasting adhesion [13].

2.2.2. Mechanical treatment

Aluminum sheets are abraded by using sand paper of 110 C to remove near-surface deformed layer. Mechanical treatment provides roughened surface in micro level, and by this surface topography modification the wettability improvement is obtained due to physicochemical variations.

2.2.3. Alkaline cleaning

Specimen aluminum sheets were put in an amount of 10 wt% Sodium Hydroxide (NaOH) solution at a temperature of 60 °C for 10 – 15 min. until white bubbles started to appear. After that, the aforementioned sheets were cleaned using hot water (40 – 45 °C) for 5 minutes to remove NaOH residues [21].

2.2.4. Chemical treatment (acidic etching)

This treatment is summarized by using forest product laboratory (FPL) according to USA standard which is mixture of 10 wt% of the inorganic compound of sodium dichromate $\text{Na}_2\text{Cr}_2\text{O}_7$, 30 wt% of H_2SO_4 (sulfuric acid) with 60 wt% distilled water. The mixture was heated to about 70 – 80 °C and immersed the aluminum sheets in this mixture for 15 minutes, then the sheets are rinsed with hot water (45 – 50 °C) for 5 minutes.

2.2.5. Electrochemical treatment (phosphoric acid anodizing) (PAA)

Anodizing is an electrochemical process for metal surface preparation to obtain strong adhesive bonding by forming porous oxide layer on the aluminum surface. This process includes immersing the aluminum sheet in an electrolyte (phosphoric acid in this study) to represent an anode of the anodizing cell and create current flow between negative cathode and positive anode electrodes. To product an anodization cell, the aluminum sheet is set as an anode while a cathode consists of a plate of stainless steel or carbon steel. Figure 1 explains the anodizing cell idea.



Figure 1. Anodization cell with electrolytic bath

When close the circuit, electrons pullout from the aluminum surface onto which they leave ions in order to produce reaction with water molecules of the electrolytic solution leading to an oxide-based layer to spread over aluminum surface as figure 2 shows [18].

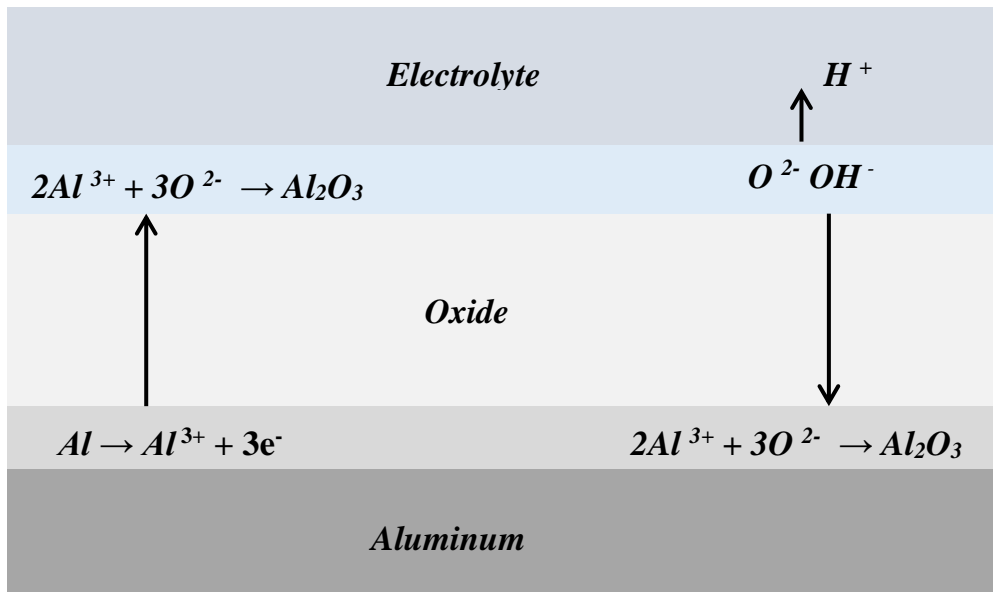


Figure 2. Aluminum / electrolyte interface schematic representation

Two types of films are formed during anodizing process barrier and porous film. Porous film is required to obtain better interfacial bonding.

Phosphoric acid anodizing process according D3933 ASTM standard was performed in this study, which can be summarized by the immersion of aluminum sheet as anode in a solution composed of 12 wt% phosphoric acid. This solution was treated with distilled water and controlled the electrolyte orthophosphoric acid (also known as phosphoric (V) acid) temperature at 23 °C for 20 – 25 min. during anodizing process. Three modes of an operating voltage were applied in this research as shown in the figure 3.

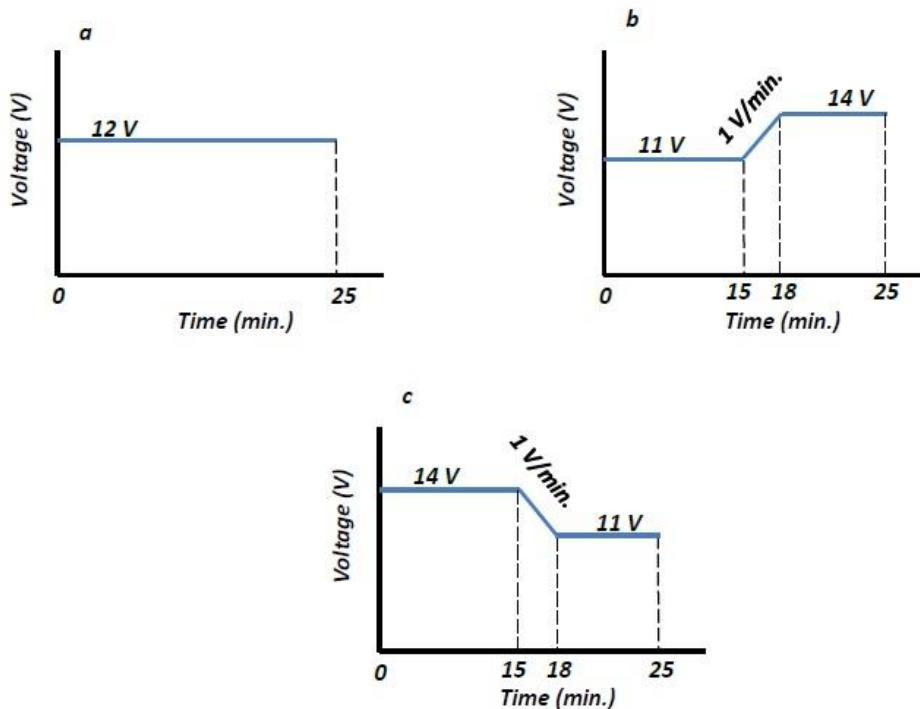


Figure 3. Operation voltage modes **a.** mode One (1) (constant voltage) & **b.** mode Two (2) (increasing voltage) **c.** mode Three (3) (decreasing voltage)

The idea behind of using different values of voltage is try to perform a modification on the pores form in porous oxide layer and the thickness of this layer. After anodizing process, the anodized aluminum sheets were rinsed by clean water (43 – 45 °C) for 10 – 15 minutes, then the aluminum sheets are dried by applying dry clean air for 30 – 40 minutes at 70°C.

2.3. Vacuum-assisted resin transfer molding technique (VARTM)

High cost autoclave composite industry was traditionally used to fabricate high performance components. This method of FML fabrication has several disadvantages such as the curing process of epoxy resin used in this manufacture process includes applying high temperature (120 – 160 °C) with high pressure (6 – 25 bar), and this causes to produce a residual stresses in the FML product [14]. Autoclave method use a prepregs which consist of fabrics impregnated with initiated resin system and partially cured until use in FML production. The resin system used in prepregs contains solvents used to keep the epoxy from curing prior to fabrication time. These solvents have high percentage of a volatile gases, therefore, it is expected that FML product has high void contents [20]. On the other hand, resin infusion in fiber layers by applying vacuum serves two functions. First, it facilitates resin flowing. Second, it provides sufficient atmospheric rate of change (gradient) of pressure to product superior-quality hybrid composite structures. And this method, (known as VARTM) has been proved to be a simple low-cost method [13]. Figure 4 explains a schematic of process utilized in fabrication GLARE specimens.

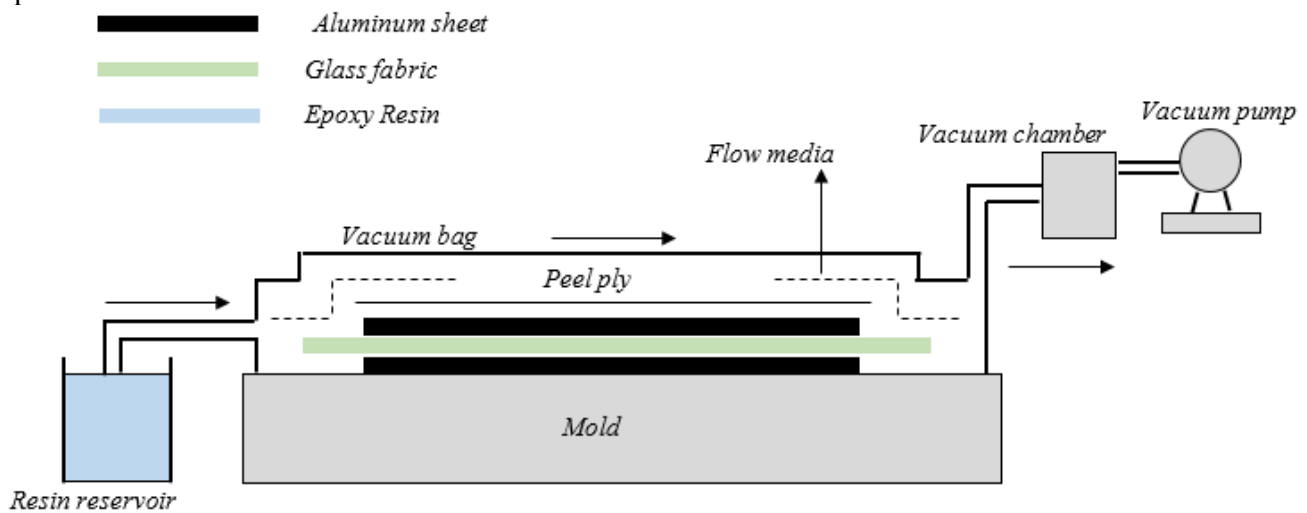


Figure 4. Schematic of VARTM set-up

This process is characterized by several advantages. Large and complex parts of FML can be fabricated during this process on the contrary of autoclave process there is limitation in the size of parts. Low viscosity, free voids and high wettability epoxy resin system is used in this process with cold curing technique therefore FML product by VARTM process is free from residual stresses and voids [14].

In this work, a suitable glass mold is cleaned by acetone from impurities before FML lay-up. Wax was placed over the mold surface to simply demold and then a peel ply layer was also applied. This layer provides hassle-free removing of the treated specimen. Aluminum sheets as well as glass fabrics were stacked in a pattern of 2/1 arrangement and then peel ply and distribution flow media were applied. The latter takes the form of a mesh layer that organizes the resin flow through thickness and length of the composite material. Spiral tubes were put at both ends (i.e. outlet & inlet) of the epoxy resin. The entire arrangement was cavorted by vacuum bag. Afterward, a pump was used to create vacuum. As the valve of the inlet opening of resin was unfastened, this low viscosity resin began streaming in spirally shaped tubes permeating through 2/1 GLARE arrangement. The fabrication of GLARE by VARTM process is shown in figure 5.

2.4. Curing process

Cross linking develops and extends to form concentrated series of polymer chains coated on the aluminum surface during curing process of epoxy resin. To obtain the best bonding of epoxy resin – hardener system with aluminum surface, the improvement rates of ring opening reactions as well as the crosslinking reactions are required [29]. In this study GLARE specimens were curing by two procedures, the first was cured at room

temperature for 24 hours. Afterwards, it was put for 15 h at 40 °C and the second 36 h at room temperature and then 4 h at 60 °C.

In this study eight sets of specimens are prepared to perform T-peel tests as shown in the table 2. The coding of each specimen in table 2 indicates first to the adopted curing process and second to the surface treatments on aluminum sheet.



Figure 5. VARTM fabrication process

2.5. Specimen preparation

The cured specimens were cut by water jet technique and prepared with respect to ASTM test method (D1876) see Figure (6) below.

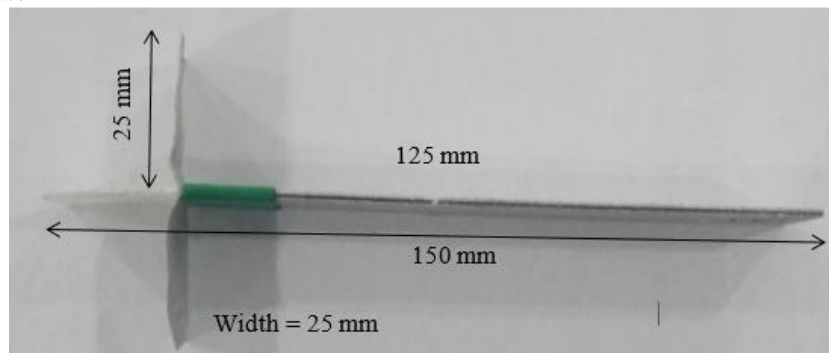


Figure 6. T-peel specimen shape with its dimensions

Table 2. Coding of Specimens Sets

Specimen No.	Curing process	Surface treatment	Coding
1	Room temperature (RT)-cured for 24 h & then 15 h under 40 °C	Mechanical only	C1-X1
2		Mechanical + Chemical + Electrochemical (Anodizing with constant voltage)	C1-X2
3		Mechanical + Chemical + Electrochemical (Anodizing with increasing voltage)	C1-X3
4		Mechanical + Chemical + Electrochemical (Anodizing with decreasing voltage)	C1-X4
5	Room temperature (RT)-cured for 36 h & then 4 h under 60 °C	Mechanical only	C2-X1
6		Mechanical + Chemical + Electrochemical (Anodizing with constant voltage)	C2-X2
7		Mechanical + Chemical + Electrochemical (Anodizing with increasing voltage)	C2-X3
8		Mechanical + Chemical + Electrochemical (Anodizing with decreasing voltage)	C2-X4



Figure 7. T-peel specimen on universal testing machine

2.6. Mechanical testing

The prepared T-peel specimens were assessed using (Model WDW – 5E, China) Microcomputer control electronic universal testing tool as shown in figure 7. The crack propagation is observed and measured continuously during testing by using digital camera was mounted on the testing machine. The specimen was marked at every 5 mm to facilitate crack lengths measurement. By using force-displacement curves obtained from the testing machine along with crack lengths measurement, the fracture energy values for all specimen sets were calculated experimentally. Fracture energy G_{IC} is calculated from the following equation [5]:

$$G_{IC} = \frac{F \cdot U}{W \cdot \Delta a} \dots \dots \dots (1)$$

(F): stands for crack-tip force while (U) represents vertical crack opening displacement, W is specimen width and Δa is crack length.

3. Results and discussion

The obtained results in this study are represented as force versus time and displacement curves of fiber metal laminate as shown in the figures 8 to 11. On the whole, the results suggest that using anodizing treatment produced a considerable improvement in adhesive strength rate of aluminum alloy sheets as well as in the fiber-reinforced epoxy layers.

The force-displacement curves of all specimens indicate that rupture has occurred after linear increasing in load and then followed by decreasing and stable in peel-force response. Generally, the specimens produced a ductility behavior pattern after linear increasing in force. This type of behavior can be explained by the fact that the initiation of the crack begins at the weaker interface. The fiber layers remain attached with a single aluminum layer at stronger interface and trace the crack route while the peel test persists. The reduction in the peeling strength is due to disturbance in force distribution observed in the width direction of the specimen, which produces shearing stresses between layers.

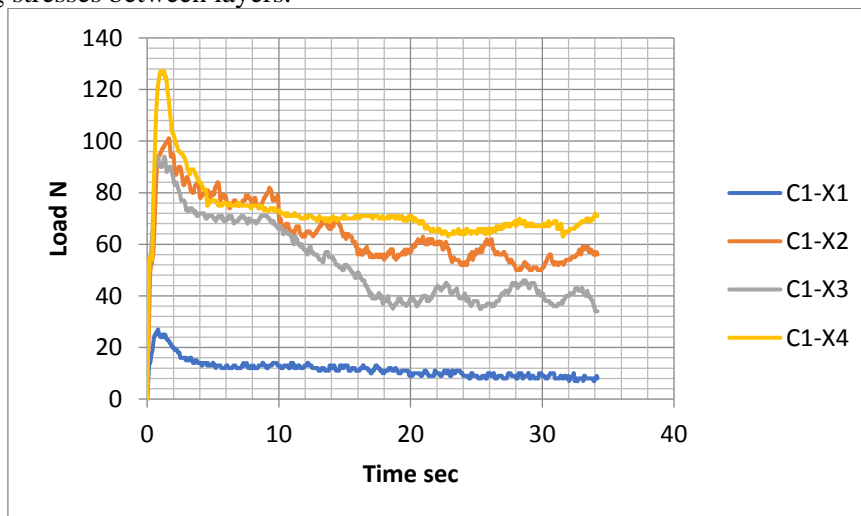


Figure 8. Load – Time curves of anodized with first procedure of curing process and unanodized specimens

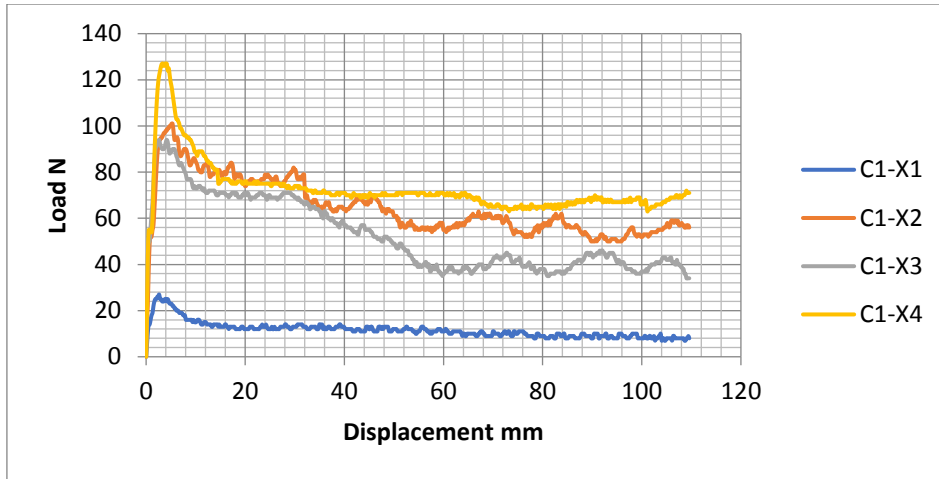


Figure 9. Load- Extension curves of anodized with first procedure of curing process and unanodized specimens

The obtain results in figures 8 to 11 show that the peak load value is the lowest for unanodized specimens with both curing process procedure (which is 26 N for the first procedure and 24 N for the second procedure). Peak load value rises to produce highest value for anodized with decreasing voltage mode-first procedure cured specimens C1-X4 (127 N).

The first procedure of curing process (24 h at room temperature and then 15 h at 40 °C) produce better performance than the second procedure (36 h at room temperature and the 4 h at 60 °C).

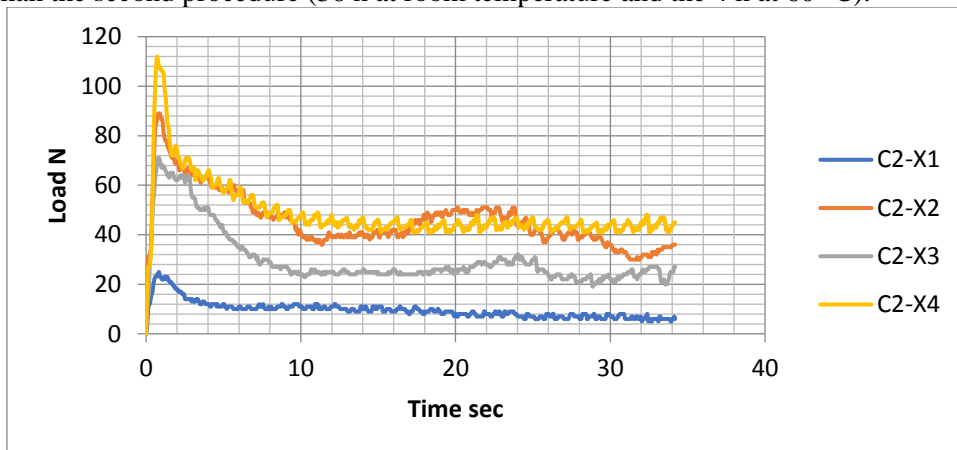


Figure 10. Load – Time curves pertaining to anodized with second procedure of curing process and unanodized specimens

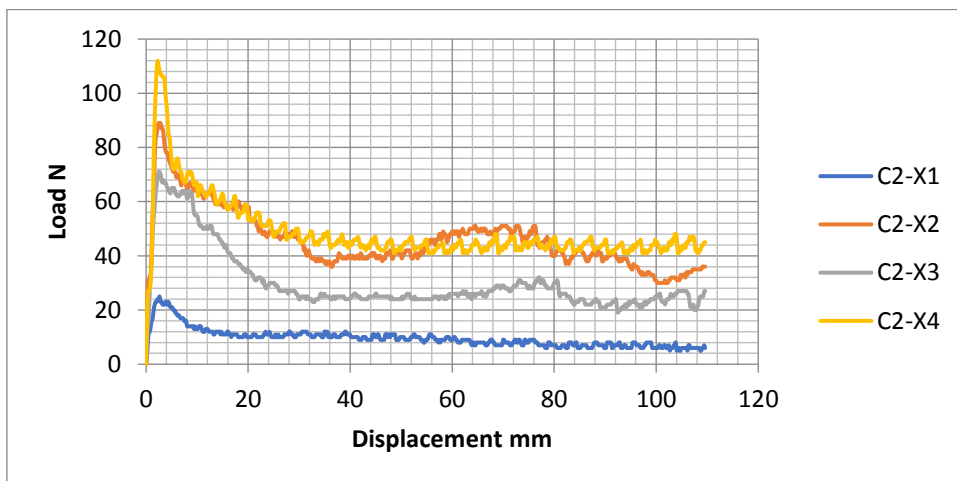


Figure 11. Load- Extension curves of anodized with second procedure of curing process and unanodized specimens

The anodizing treatment with decreasing voltage mode offered better improvement in bonding strength (specimens C1-X4 and C2-X4) because this surface treatment on aluminum sheets create funneled morphologies as shown in figure 12 which consists of an external area with rather rough pores diameter so as to enhance epoxy penetration and internal area that has thin pores diameter to enhance oxide layer stability. This transition between two regions may prevent an interfacial mechanical stresses.

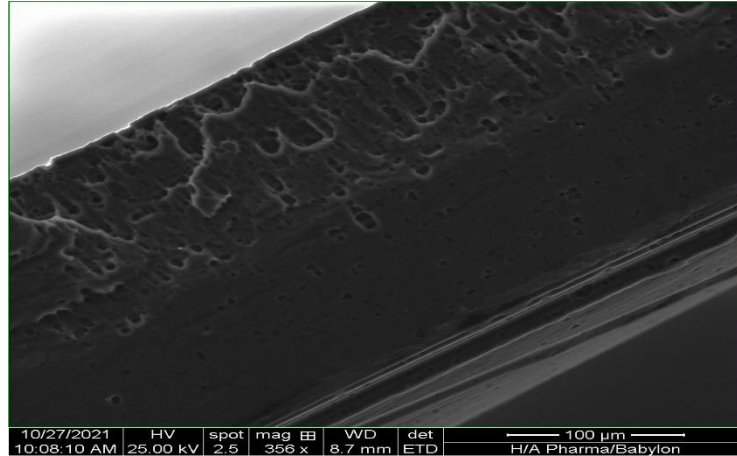


Figure 12. A revolved (Cross-sectional) view of the (AAO) layer laid over T3 temper 2024 aluminum via PAA with decreasing voltage mode

Lowest improvement is obtained from anodizing treatment with increasing voltage mode (specimens C1-X3 and C2-X3). This is due to the aluminum surface morphology is reversed to produce pores with small diameter as shown in figure 13, and this results in the difficulty of the epoxy penetration through porous oxide layer.

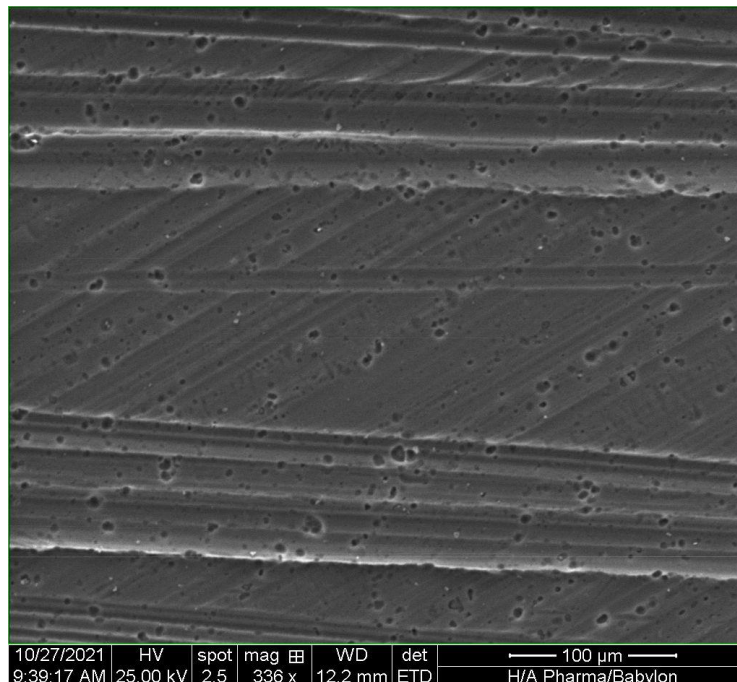


Figure 13. Surface morphology for anodized specimen with increasing voltage mode

Three specimens are tested for each set of surface condition and curing which have been shown in table 2 and find out the average values from the obtained results and listed in table 3. C1-X4 specimens possess highest fracture energy and this due to good interfacial adhesion between aluminum surface and fiber-epoxy layer which is produced as a result of anodizing treatment especially with decreasing and constant voltage modes. Anodizing process creates porous oxide layer on aluminum surface as shown in figure 14, which improves epoxy penetration and surface wettability. This process yields mechanical interlock mechanism with good interface adhesive bonding of GLARE laminates manufactured using VARTM.

Table 3. Experimental T-peel test (ASTM D1876) results

Specimen coding	Peak Force (PF) (Newton metres)	Crack opening (mm)	Fracture energy G_{IC} (J/m ²)
C1-X1	26	2.442	572.03
C1-X2	101	4.749	4349.03
C1-X3	94	2.634	2912.66
C1-X4	127	3.406	5155.22
C2-X1	24	2.447	519.73
C2-X2	89	2.447	2747.78
C2-X3	71	2.455	2741.96
C2-X4	112	2.270	3350.15

C1-X1 and C2-X1 specimens offered peak loads values 6 times and fracture energy 9 times lesser than C1-X4 specimens. The absence of non-anodic oxide layer resulted in the weak interfacial bonding.

An important characteristics of the anodization treatment is that increasing of surface wettability and create nano scale surface morphology. This feature provides good bonding between aluminum and glass fiber layers.

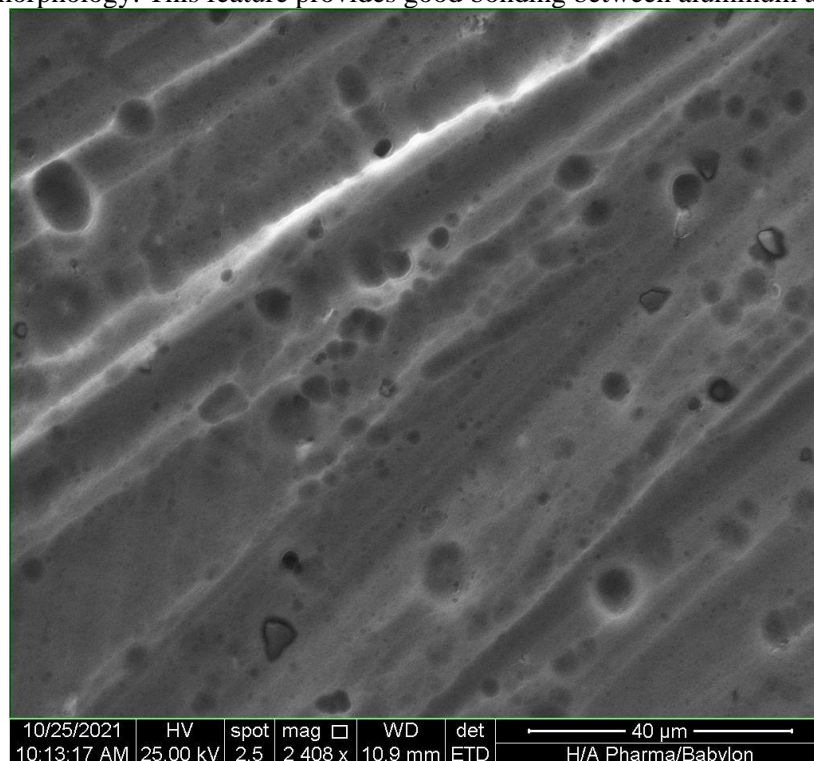


Figure 14. Porous oxide layer produced by anodizing process

Figure 15 shows that the failure which was occurred in unanodized specimens (C1-X1 and C2-X1) is an adhesive failure because no epoxy remains of the epoxy rich layer on aluminum surface. While the anodized specimens with all voltage modes has offered highest bonding with failure combination of fiber rich cohesive failure and epoxy cohesive failure, therefore this gives high peak load and raise the level of stabilized load curve.

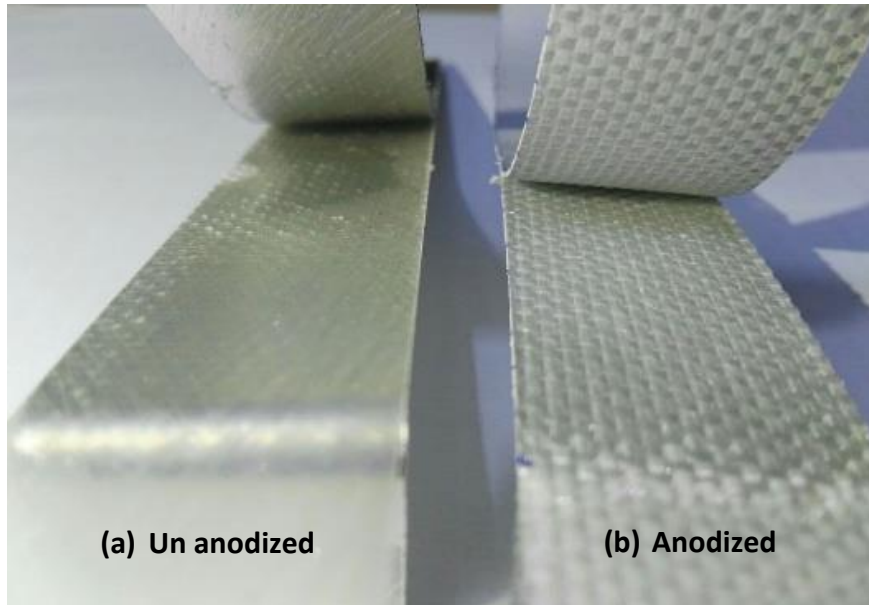


Figure 15. De-bonded surface comparison for peeling areas: (a) Un-anodized; (b) Anodized specimens

4. Numerical simulation

In order to verify the delamination behavior which has been observed from experimental results, Abaqus 2017 software was used to implement numerical simulation of C1-X4 specimen. Two dimensional, planar, deformable (employing shell as a base) parts were created according to the dimension and boundary conditions shown in the figure 16.

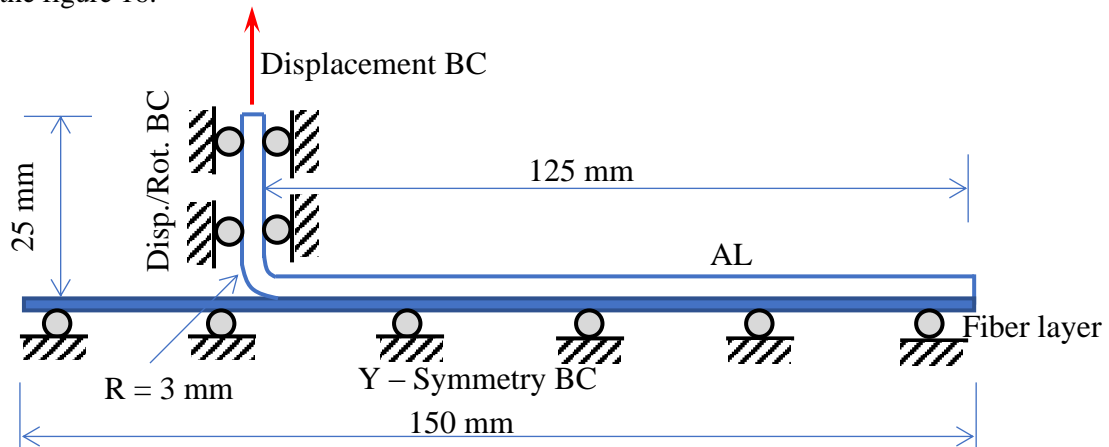


Figure 16. Dimensions and boundary conditions of FML specimen

For aluminum layer, elastic properties ($E = 72.4$ GPa & Poisson's ratio $\mu = 0.33$) and plastic properties (stress with plastic strain) were obtained from tensile test data. Due to the simulation objective is the cohesive failure in very thin adhesive layer, the glass fiber layer is modeled as elastic isotropic material ($E = 33$ GPa and Poisson's ratio = 0.3). For adhesive bonding, very thin cohesive layer with traction property ($E/E_m = 3740$ GPa, $G_1/E_{ss} = 1370$ GPa and $G_2/E_{tt} = 1370$ GPa according to the supplier data) is adopted. Damage initiation according to traction/separation law - maximum stress damage criterion and fracture energy G_{IC} are used to matching load-displacement curves of experimental and numerical data.

Aluminum, glass fiber and cohesive layers are interacted by tie constraints. Plane stress, structural, linear, quadrilateral and with reduced integration elements type CPS4R are used to mesh aluminum and glass fiber parts. While cohesive, structural and linear elements type COH2D4 are used to mesh adhesive layer which is very thin layer approach to zero. The total number of model elements is 7436 which consist of 3780 element for aluminum layer, 1856 element for glass fiber layer and 1800 element for cohesive layer as shown in the figures 17 and 18.

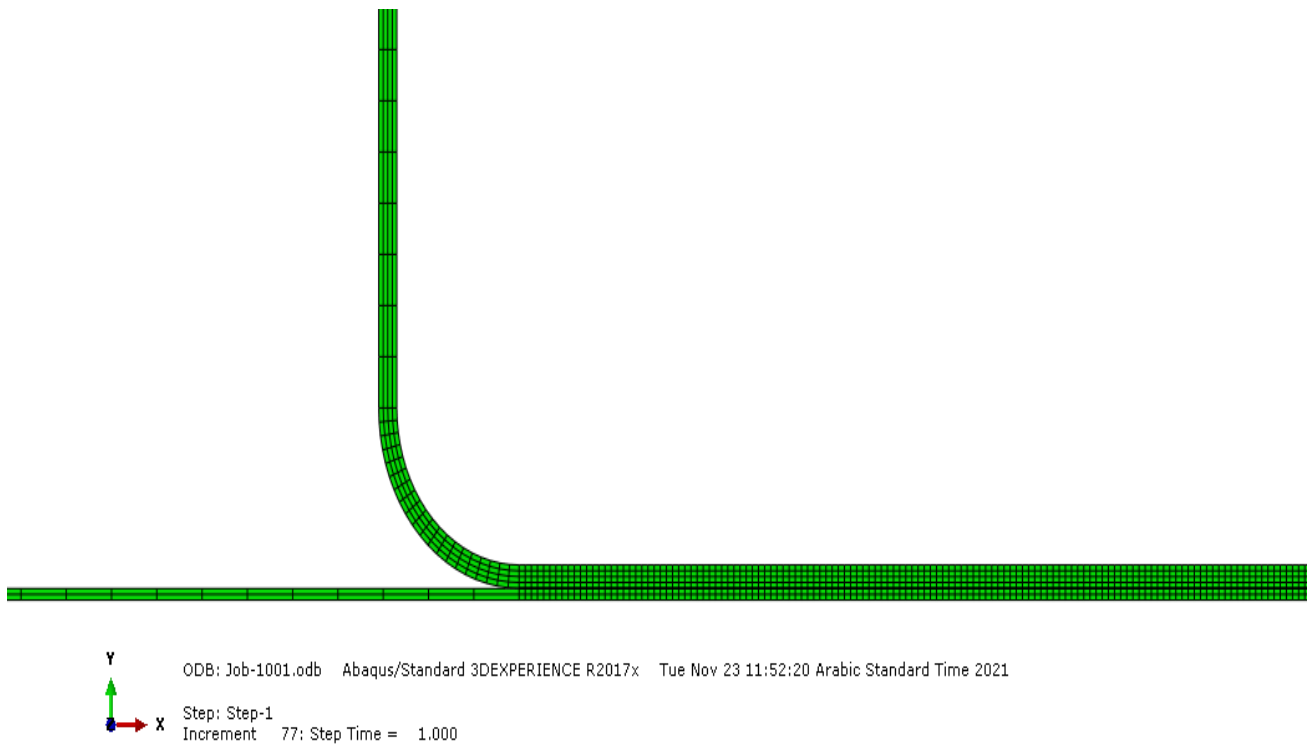


Figure 17. Meshing of model consist of aluminum layer and glass fiber layer

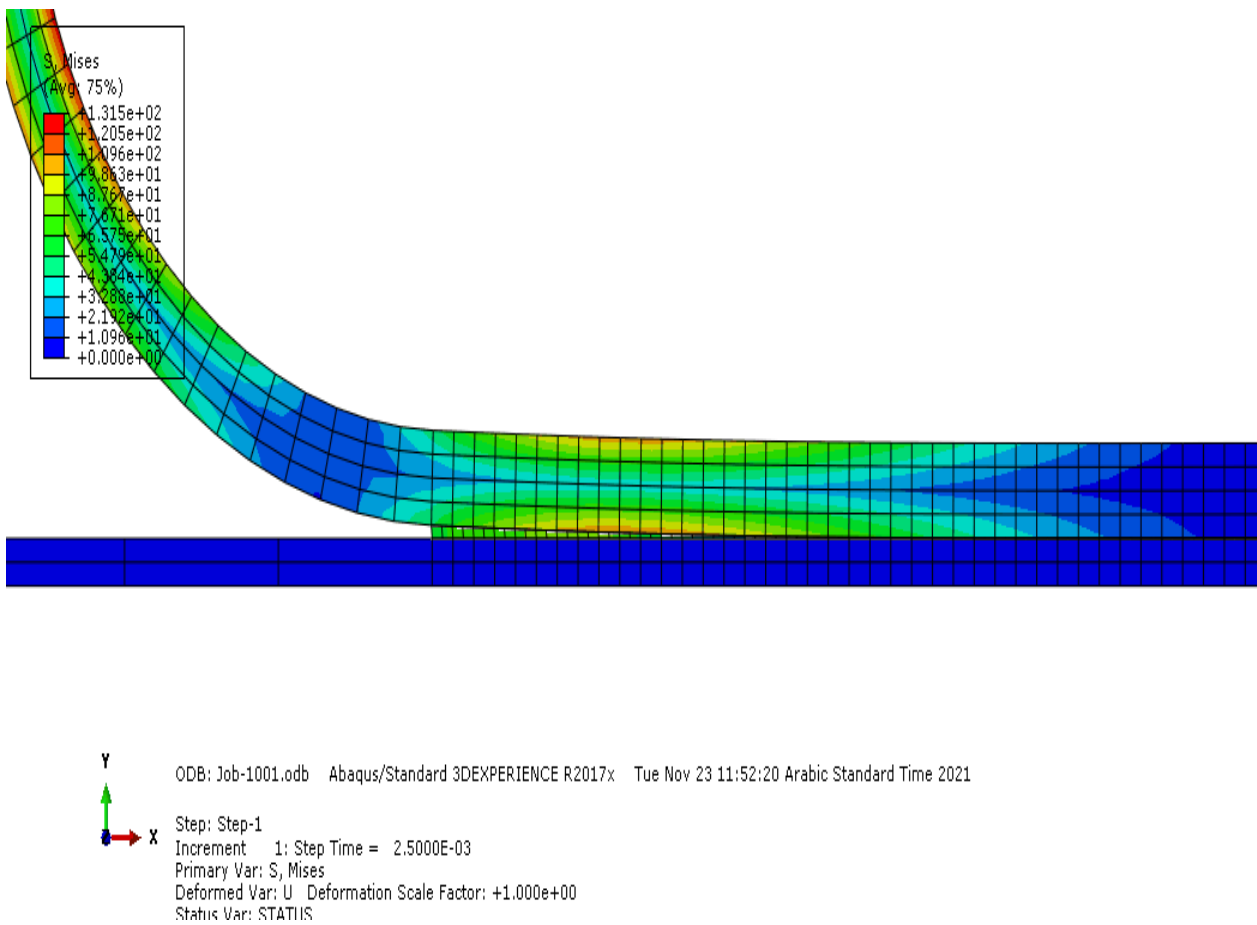


Figure 18. The model with stress gradient

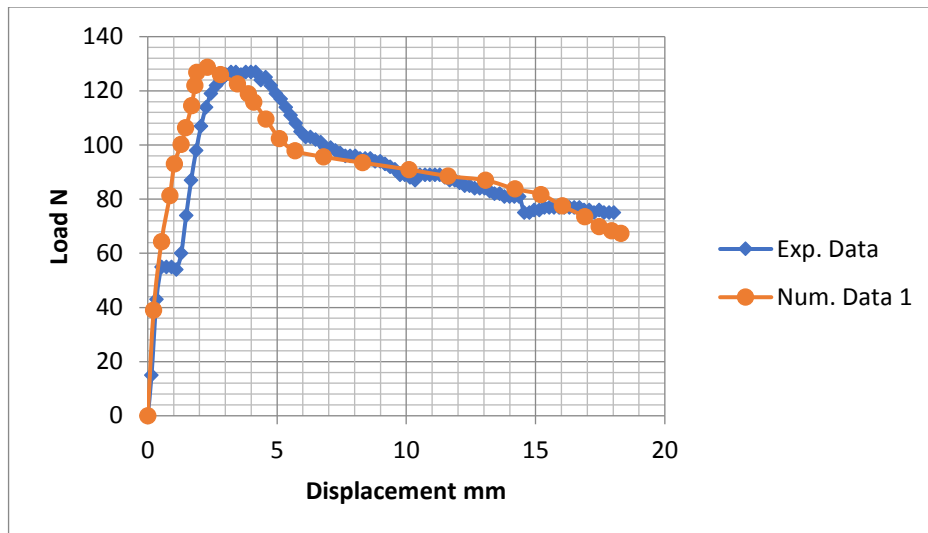


Figure 19. Numerical and experimental load – displacement curves

The value of load – Extension (displacement) curve was calculated using this simulation for C1-X4 specimen. This was put in comparison with that of experimental load – extension curve for this specimen as shown in figure 19. From these curves, there is congruence in specimen behavior for both results (i.e. numerical & experimental).

5. Conclusion

The enhancement procedures that this study adopted as regards the manufacturing of glass laminate aluminum reinforced epoxy GLARE by using VARTM technique explain that interfacial bonding can be improved through both anodizing process with all voltage modes and curing method. The curing and post curing procedures has a good effect of increasing epoxy resin strength, while it has a medium effect on interlaminar shear strength of aluminum alloy as well as fiber glass layers. Anodizing is instrumental in the modification the aluminum surface morphology and produces a significant interlocking between aluminum sheets and fiber layers. Due to the modification in shape and diameter of pores in oxide layer, the specimens which manufactured by anodizing process with decreasing voltage mode and cured by the first procedure offer highest peak load, mode I fracture toughness and stabilized load level. From the obtained results, the manufacturing process used for C1-X4 specimens set is the recommended one.

References

- [1] A. Salve, R. Kulkarni and A. Mache, "A review: Fiber metal laminates (FML's) – Manufacturing, test methods and numerical modeling," *International Journal of Engineering Technology and Sciences (IJETS)*, vol. 6, no. 1, pp. 71-84, 2016.
- [2] K. Logesh, V. K. Bupesh Raja, V. H. Nair, Sreerag K. M., Vishvesvaran K.M and M. Balaji, "Review on manufacturing of fiber metal laminates and its characterization techniques," *International Journal of Mechanical Engineering and Technology (IJMET)*, vol. 8, no. 10, pp. 561-578, 2017.
- [3] D. Lehmhus, A. von Hehl, J. Hausmann, K. Kayvantash, R. Alderliesten and J. Hohe, "New materials and processes for transport applications: going hybrid and beyond," *Advanced Engineering Materials*, pp. 1-7, 2018.
- [4] E. Sherkatghanad, L. Lang, H. Blala, Lei Li and S. Alexandrov, "Fiber metal laminate structure, a good replacement for monolithic and composite materials," *Materials science and Engineering*, vol. 576 pp. 1-9, 2019.
- [5] F. Khan, F. Qayyum, W. Asghar, M. Azeem, Z. Anjum, A. Nasir and Masood Shah, "Effect of various surface preparation techniques on the delamination properties of vacuum infused Carbon fiber reinforced aluminum laminates (CARALL): Experimentation and numerical simulation," *Journal of Mechanical Science and Technology*, vol. 31, no.11, pp. 5265-5272, 2017.

- [6] T. Subesh, D. Yogaraj and V. Ramesh, "Characterization of fiber metal laminates, bonding and manufacturing methods," *International Journal of Innovative Technology and Exploring Engineering (IJITEE)*, vol.8, no. 11, pp.1062-1065, 2019.
- [7] W. Asghar, M. A. Nasir, F. Qayyum, M. Shah, M. Azeem, S. Nauman and S. Khushnood, "Investigation of fatigue crack growth rate in CARALL, ARALL and GLARE," *Fatigue and Fracture Engineering Materials and Structures*, pp.1-15, 2016.
- [8] S. Bhat and S. Narayanan, "On fabrication and testing of GLARE," *ARPN Journal of Engineering and Applied Sciences*, vol. 9, no. 9, pp. 1606-1614, 2014.
- [9] Ion Dinca, A. Stefan and Ana Stan, "Aluminum/glass fibre and aluminum/carbon fibre hybrid laminates," *INCAS Bulletin*, vol. 2, no. 2, pp. 33-39, 2010.
- [10] L.B. Vogelesang and A. Vilot, "Development of fiber metal laminates for advanced aerospace structures," *Journal of Materials Processing Technology*, vol. 103, pp. 1-5, 2000.
- [11] N. A. Patil, S. S. Mulik, K. S. Wangikar and A. P. Kulkarni, "Characterization of glass laminate aluminum reinforced epoxy-A review," *Procedia Manufacturing*, vol. 20, pp. 554-562, 2018.
- [12] T. Sinmazcelik, E. Avcu, M. Ozgur Bora and O. Coban, "A review: Fiber metal laminates, background, bonding types and applied test methods," *Materials and Design*, vol. 32, pp. 3671-3685, 2011.
- [13] H. Qaiser, S. Umar, A. Nasir, M. Shah and S. Nauman, "Optimization of interlaminar shear strength behavior of anodized and unanodized ARALL composites fabricated through VARTM process," *Int J Mater Form*, pp. 1-13, 2014.
- [14] G. Tuncol, "Modeling the vacuum assisted resin transfer molding (VARTM) process for fabrication of fiber/metal hybrid laminates," *Dissertation, Michigan State University*, 2010.
- [15] O. de Mendibil, L. Aretxabaleta, M. Sarrionandia, M. Mateos and J. Aurrekoetxea, "Impact behaviour of glass fibre-reinforced epoxy/aluminium fibre metal laminate manufactured by Vacuum Assisted Resin Transfer Moulding," *Composite Structures*, vol. 140, pp. 118-124, 2016.
- [16] P. Hergan, Yanxiao Li, L. Zaloznik, B. Kaynak and F. Arbeiter, "Using (VA)RTM with a rigid mould to produce fiber metal laminates with proven impact strength," *Journal of Manufacturing and Materials Processing*, vol. 2, no. 38, pp. 1-12, 2018.
- [17] M. A. Agwa, S. M. Youssef, S. S Ali-Eldin and M. Megahed, "Integrated vacuum assisted resin infusion and resin transfer molding technique for manufacturing of nano-filled glass fiber reinforced epoxy composite," *Journal of Industrial Textiles*, vol. 0, no. 0, pp. 1-32, 2020.
- [18] S. T. Abrahami, J. M. M. de Kok, H. Terryn and Johannes M. C. Mol, "Towards Cr(VI)-free anodization of aluminum alloys for aerospace adhesive bonding applications: A review," *Front. Chem. Sci. Eng.*, pp. 1-18, 2017.
- [19] S. Y. Park, W. J. Choi, H. Soap Choi, H. Kwon and S. Hwan Kim, "Recent Trends in surface treatments technologies for airframe adhesive bonding processing: A review," *The Journal of Adhesion*, vol. 86, pp. 192-221, 2010.
- [20] S. Y. Park, W. J. Choi, H. Soap Choi and H. Kwon, "Effects of surface pre-treatment and void content on GLARE laminate process characteristics," *Journal of Materials Processing Technology*, vol. 210, pp. 1008-1016, 2010.
- [21] D. Giridharan and B. Rakham, "Experimental analysis of fiber metal laminates," *Materials Science and Engineering*, vol. 455, pp.1-15, 2018.
- [22] N. Karunakaran and A. Rajadurai, "Effect of surface treatment on mechanical properties of glass fiber/stainless steel wire mesh reinforced epoxy hybrid composites," *Journal of Mechanical Science and Technology*, vol. 30, no. 6, pp. 2475-2482, 2016.
- [23] Y. Chen, Y. Wang and Hui Wang, "Research progress on interlaminar failure behavior of fiber metal laminates," *Advances in Polymer Technology*, pp. 1-20, 2020.
- [24] J. G. Carrillo and W.J. Cantwell, "Mechanical properties of a novel fiber-metal laminate based on a polypropylene composite," *Mechanics of Materials*, vol. 41, pp. 828-838, 2008.
- [25] C. Bellini, V. Di Cocco, F. Iacoviello and L. Sorrentino, "Influence of structural characteristics on the interlaminar shear strength of CFRP/Al fibre metal laminates," *Procedia Structural Integrity*, vol. 18, pp. 373-378, 2019.
- [26] U. Tamilarasan, L. Karunamoorthy and K. Palanikumar, "Mechanical properties evaluation of the carbon fibre reinforced aluminium sandwich composites," *Materials Research*, vol. 18, no. 5, pp. 1029-1037, 2015.

- [27] E. Valdés, J. D. Mosquera-Artamonov, C. Cruz-Gonzalez and J. Jaime Taha-Tijerina, "Multiobjective optimization on adhesive bonding of aluminum-carbon fiber laminate," *Computational Intelligence*, pp. 1-14, 2021.
- [28] M. Paz Martinez-Viademonte, S. T. Abrahami, T. Hack, M. Burchardt and H. Terryn, "A Review on anodizing of aerospace aluminum alloy for corrosion protection, *Coatings*," vol. 10, pp. 1-30, 2020.
- [29] Verbruggen MLCE, "Aramid reinforced aluminum laminates," Dissertation, Faculty of Aerospace Engineering, Delft University of Technology, 1987.